

Novel Nitro-PAH Formation from Heterogeneous Reactions of PAHs with NO₂, NO₃/N₂O₅, and OH Radicals: Prediction, Laboratory Studies and Mutagenicity

The Faculty of Oregon State University has made this article openly available. Please share how this access benefits you. Your story matters.

Citation	Jariyasopit, N., McIntosh, M., Zimmermann, K., Arey, J., Atkinson, R., Cheong, P. H. Y., ... & Massey Simonich, S. L. (2014). Novel Nitro-PAH Formation from Heterogeneous Reactions of PAHs with NO ₂ , NO ₃ /N ₂ O ₅ , and OH Radicals: Prediction, Laboratory Studies, and Mutagenicity. <i>Environmental Science & Technology</i> , 48(1), 412-419. doi:10.1021/es4043808
DOI	10.1021/es4043808
Publisher	American Chemical Society
Version	Accepted Manuscript
Terms of Use	http://cdss.library.oregonstate.edu/sa-termsofuse

1 **Novel Nitro-PAH Formation from Heterogeneous Reactions of PAHs with NO₂, NO₃/N₂O₅,**
2 **and OH Radicals: Prediction, Laboratory Studies and Mutagenicity**

3 NARUMOL JARIYASOPIT¹, MELISSA MC INTOSH¹, KATHRYN ZIMMERMANN², JANET AREY², ROGER
4 ATKINSON², PAUL HA-YEON CHEONG¹, RICH G. CARTER¹, TIAN-WEI YU³, RODERICK H.
5 DASHWOOD³, STACI L. MASSEY SIMONICH^{1,4*}

6 ¹Department of Chemistry, Oregon State University, Corvallis, Oregon USA 97331; ²Air Pollution Research Center,
7 University of California, Riverside; ³Institute of Biosciences & Technology, Texas A&M Health Science Center,
8 Houston, Texas, USA, 77030; ⁴Environmental and Molecular Toxicology, Oregon State University, Corvallis,
9 Oregon, USA, 97331.

10 *Corresponding author e-mail: staci.simonich@orst.edu; phone: (541) 737-9194; fax: (541) 737-
11 0497

12 **Abstract**

13 The heterogeneous reactions of benzo[a]pyrene-d₁₂ (BaP-d₁₂), benzo[k]fluoranthene-d₁₂
14 (BkF-d₁₂), benzo[ghi]perylene-d₁₂ (BghiP-d₁₂), dibenzo[a,i]pyrene-d₁₄ (DaiP-d₁₄), and
15 dibenzo[a,l]pyrene (DalP) with NO₂, NO₃/N₂O₅, and OH radicals were investigated at room
16 temperature and atmospheric pressure in an indoor Teflon chamber and novel mono NO₂-DaiP,
17 and mono NO₂-DalP products were identified. Quartz fiber filters (QFF) were used as a reaction
18 surface and the filter extracts were analyzed by GC/MS for nitrated-PAHs (NPAHs) and tested in
19 the Salmonella mutagenicity assay, using *Salmonella typhimurium* strain TA98 (with and without
20 metabolic activation). In parallel to the laboratory experiments, a theoretical study was
21 conducted to rationalize the formation of NPAH isomers based on the thermodynamic stability of
22 OH-PAH intermediates, formed from OH-radical-initiated reactions. NO₂ and NO₃/N₂O₅ were
23 effective oxidizing agents in transforming PAHs to NPAHs, with BaP-d₁₂ being the most readily
24 nitrated. Reaction of BaP-d₁₂, BkF-d₁₂ and BghiP-d₁₂ with NO₂ and NO₃/N₂O₅ resulted in the
25 formation of more than one mono-nitro isomer product, while the reaction of DaiP-d₁₄ and DalP
26 resulted in the formation of only one mono-nitro isomer product. The direct-acting mutagenicity
27 increased the most after NO₃/N₂O₅ exposure, particularly for BkF-d₁₂ in which di-NO₂-BkF-d₁₀
28 isomers were measured. The deuterium isotope effect study suggested that substitution of

29 deuterium for hydrogen lowered both the direct and indirect acting mutagenicity of NPAHs and
30 may result in an underestimation of the mutagenicity of the novel NPAHs identified in this study.

31 **Introduction**

32 Nitroated polycyclic aromatic hydrocarbons (NPAHs) are PAH derivatives emitted
33 directly to the atmosphere from combustion sources and/or formed from atmospheric
34 transformation via homogeneous gas-phase OH- and NO₃-radical initiated reactions of PAHs,¹
35 and some NPAHs are more mutagenic than the parent PAHs.^{2, 3} Gas-phase reactions of PAHs to
36 form NPAHs are initiated by either OH or NO₃ radical attack at the position of highest electron
37 density on the aromatic ring, followed by NO₂ addition with subsequent loss of H₂O or HNO₃,
38 respectively. In contrast, heterogeneous nitration may follow a different mechanism and
39 previous studies have shown that heterogeneous reactions of pyrene and fluoranthene with
40 NO₃/N₂O₅ yield different nitropyrene and nitrofluoranthene isomers than do the corresponding
41 gas-phase reactions.⁴⁻⁷ The kinetics of heterogeneous reactions vary significantly due to the
42 inherent complexity of heterogeneous reactions caused by the characteristics of the substrates,
43 surface chemistry and the substrate-specific kinetics of heterogeneous reactions.⁸⁻¹¹ The
44 formation of NPAHs from the heterogeneous reactions of PAHs containing two to five rings has
45 been studied with NO₂, N₂O₅,^{5-7, 10, 12-15} whereas a limited number of studies have investigated
46 the formation of NPAHs from the heterogeneous reaction of PAHs with more than five aromatic
47 rings.¹⁶ In field studies, nitrobenzopyrenes and nitroperylene (MW297) were the highest
48 molecular weight NPAHs detected in the atmosphere.^{17, 19-20}

49 The objectives of this study were to 1) identify NPAHs, including novel NPAHs, formed
50 from the heterogeneous reaction of filter-sorbed, low volatility perdeuterated PAHs with NO₂,
51 NO₃/N₂O₅, and OH radicals using laboratory experiments and theoretical calculations and 2)

52 associate NPAH formation in the laboratory experiments with the mutagenicity of the extracts.
53 Five higher molecular weight PAHs, including benzo[a]pyrene-d₁₂ (BaP-d₁₂),
54 benzo[k]fluoranthene-d₁₂ (BkF-d₁₂), benzo[ghi]perylene-d₁₂ (BghiP-d₁₂), dibenzo[a,i]pyrene-d₁₄
55 (DaiP-d₁₄), and dibenzo[a,l]pyrene (DalP) were selected for this research because of their
56 mutagenicity^{21, 22} and the lack of data on their formation of NPAH products during
57 heterogeneous reactions. Deuterated PAHs were used for the experiments, except for DalP for
58 which the deuterated analog was not commercially available, because they are not present in the
59 environment and allowed us to attribute the formation of deuterated nitro PAH products solely to
60 the reactions in the chamber. Because the mutagenicity of deuterated nitro PAH products may
61 differ from non-deuterated analogs, a deuterium isotope effect study was carried out to
62 investigate the effect of perdeuteration on mutagenicity. To our knowledge, NPAH products of
63 DalP and DaiP have not been previously identified.

64 **Experimental**

65 **Chemicals and Materials.** Perdeuterated BaP-d₁₂, BkF-d₁₂, BghiP-d₁₂, and DaiP-d₁₄ were
66 purchased from CDN Isotopes (Point-Claire, Quebec, Canada) and Cambridge Isotope
67 Laboratories (Andover, MA). Because perdeuterated DalP was not commercially available we
68 purchased the non-deuterated DalP from Cambridge Isotope Laboratories (Andover, MA).
69 Dichloromethane, ethyl acetate and dimethyl sulfoxide were purchased from Fisher Scientific
70 (Santa Clara, CA) and EMD Chemicals (Gibbstown, NJ). Salmonella tester strain TA98 was
71 originally purchased from Xenometrix, Inc. Of the mono-NO₂-PAH and di-NO₂-PAH products
72 identified in this study, only 6-NO₂-BaP-d₁₁ was commercially available and was purchased
73 from Chiron AS (Trondheim, Norway). Details of the synthesis of 7-nitrobenzo[k]fluoranthene,

74 3,7-dinitrobenzo[k]fluoranthene, 7-nitrobenzo[ghi]perylene and 5-nitrobenzo[ghi]perylene are
75 given in Supporting Information (SI).

76 **Spiked Filter Preparation and Exposures.** Heterogeneous reactions of particulate-bound
77 PAHs have been observed in chamber studies and in the ambient atmosphere^{5-7, 23}. In this study,
78 the quartz fiber filters (QFFs) (8 in x 10 in, No.1851-865, Tisch Environmental, Cleves, OH)
79 were pre-baked (350°C) before use. Each clean QFF was cut into 4 quarters. Ten µg of the
80 individual PAHs in ethyl acetate were deposited separately onto each quarter of the QFFs with a
81 pipette and placed in the laboratory fume hood, allowing ethyl acetate to evaporate at room
82 temperature for approximately 30 minutes. A quarter of clean, unspiked QFF was also placed in
83 the chamber during each experiment as a negative control for toxicological and chemical studies.

84 Laboratory experiments were carried out in ~7000 L indoor collapsible Teflon chamber
85 equipped with two parallel banks of black lamps and a Teflon-coated fan at room temperature
86 (~297 K) and ~740 Torr.⁷ All the filters were placed on a standing, rotating apparatus inside the
87 Teflon chamber.⁵ Details of how NO₂, NO₃/N₂O₅, and OH radicals were generated are given in
88 SI.

89 **Sample extraction and Analysis.** The QFFs were extracted twice with pressurized liquid
90 extraction and dichloromethane using an extraction method previously described in detail¹⁸ and
91 both extracts were combined. The extracts that were subjected to chemical analysis were
92 evaporated and solvent-exchanged to ethyl acetate under a purified N₂ stream with a Turbovap II
93 (Caliper Life Sciences, MA). The extracts subjected to the Salmonella assay were evaporated to
94 dryness under a stream of N₂ and the residue was dissolved in 500 µl of dimethylsulfoxide
95 (DMSO). The extracts from the unexposed filters, that had been spiked with individual PAH,

96 were split in half based on solvent weight. One half of the extract was prepared for mutagenicity
97 testing and the other half was prepared for chemical analysis.

98 The analyses of parent PAHs and NPAHs in the analytical extracts were conducted using
99 gas chromatographic mass spectrometry (GCMS, Agilent 6890 GC coupled with an Agilent
100 5973N MSD) in selected ion monitoring (SIM) and scan modes using both electron impact (EI)
101 and negative chemical ionization (NCI) (using CH₄ as the reagent gas), with a programmed
102 temperature vaporization (PTV) inlet (Gerstel, Germany). A 5% phenyl substituted
103 methylpolysiloxane GC column (DB-5MS, 30m×0.25mm I.D., 0.25 μm film thickness, J&W
104 Scientific, USA) was used to separate the parent PAHs and NPAHs.

105 **Theoretical Study.** In parallel to the laboratory experiments, a theoretical study was
106 conducted using Density Functional Theory (DFT), with the B3LYP functional and the 6-31G(d)
107 basis set, as implemented in Gaussian03. The thermodynamic stability of the OH-PAH
108 intermediates was used to rationalize the formation of NPAH isomers. From our computations,
109 we used the thermodynamic stability of various isomeric OH-PAH intermediates to predict the
110 regioselectivity of heterogeneous nitration (see discussion below).

111 **Salmonella Mutagenicity Assay.** The basic method followed that reported by Maron and
112 Ames²⁴ and *Salmonella typhimurium* strain TA98 was used in the study. The experimental details
113 have been described elsewhere.¹⁸ The positive control doses were 2 μg of 2-aminoanthracene (2-
114 AA) and 20 μg of 4-nitro-1,2-phenylenediamine (NPD) for assays with and without metabolic
115 activation (rat S9 mix), respectively. The negative control (DMSO) dose was 30 μl. All filter
116 extracts were tested in triplicate.

117 **Results and Discussion**

118 **Theoretical Studies.** The mechanism of gas-phase OH radical-initiated reaction with PAHs
119 to give NPAH has been previously described.^{1, 4, 7, 25, 26} Scheme 1 shows that, in the gas-phase,
120 the initial addition of OH radical to an aromatic ring leads to an OH-PAH adduct. This radical
121 may react with NO₂ to yield a nitrocyclohexadienyl radical intermediate, followed by water
122 elimination to form the NPAH. Alternatively, in ambient atmospheres, the OH-PAH adduct can
123 also react with O₂ to give other products.²⁶

124 To verify our computation strategy, computations for pyrene and fluoranthene were
125 carried out and compared with nitro products identified in a previous gas-phase OH-radical
126 chamber study⁴ (Table SI.1). Positions 1 and 3 on pyrene and fluoranthene, respectively, were
127 found to yield the most thermodynamically stable OH-PAH adduct intermediates (pyrene: ΔG_{rxn}
128 = -18.4 kcal/mol and fluoranthene: ΔG_{rxn} = -16.7 kcal/mol) (Table SI.1). Followed by NO₂
129 addition to the *ortho* position, the reactions were predicted to yield 2-nitropyrene and 2-
130 nitrofluoranthene as major NPAH products from the OH radical-initiated gas-phase reaction of
131 pyrene and fluoranthene, respectively. The good agreement between the computed and
132 experimental results⁴ for pyrene and fluoranthene suggested that the thermodynamic stability of
133 the OH-PAH adducts in the first step of the gas-phase OH radical-initiated reaction could be
134 used to predict the formation of NPAHs in the gas-phase.

135 The strong thermodynamic stability of intermediates formed from addition to 1 and 3
136 positions on pyrene and fluoranthene, respectively, dictates all reactions. Therefore, addition of
137 NO₂ by direct nitration reactions should also occur at the same positions. Unlike the gas-phase
138 radical-initiated reactions, the heterogeneous nitration of pyrene and fluoranthene with N₂O₅⁶
139 and NO₂^{12, 27} formed 1-nitropyrene and 3-nitrofluoranthene as dominant isomers. Although the
140 isomer distributions of nitropyrenes and nitrofluoranthenes can be used to distinguish between

141 the radical-initiated and heterogeneous reactions and possible reaction mechanisms have been
142 previously discussed^{5-6, 13, 28}, the reaction mechanism of heterogeneous nitration has not been
143 unequivocally identified. Table 1 shows the calculated free energies of the OH-PAH adducts for
144 all possible OH radical attack positions at peripheral aromatic carbons and predicts the NPAHs
145 formed from heterogeneous reaction of BaP, BkF, BghiP, DaiP, and DalP. The optimized
146 geometries and energies of the studied PAHs and intermediates are given in the SI.

147 **NPAH Product Identification.** All major NPAH product isomers, with peak height in the
148 GC chromatograms greater than three times the noise peak height, were identified based on the
149 GC retention time and full scan EI and/or NCI mass spectra of the standards when they were
150 commercially available. In addition, we synthesized 7-nitrobenzo[k]fluoranthene, 3,7-
151 dinitrobenzo[k]fluoranthene, 7-nitrobenzo[ghi]perylene and 5-nitrobenzo[ghi]perylene because
152 they were not commercially available (see the SI). Table 1 lists the NPAHs identified in the
153 laboratory exposure experiments and whether or not they had been previously detected in the
154 environment.

155 For NPAH isomers without available standards, a previously published method was used to
156 predict their GC retention time orders.²⁹ White et al. found that the dipole moment of mono-
157 nitro PAH isomers predicted their GC retention time order on a non-polar SE-52 GC column, a
158 5% phenyl substituted methylpolysiloxane stationary phase, with the NPAH isomers eluting in
159 order of increasing dipole moment.²⁹ In this study, we predicted the GC retention time orders of
160 the most stable mono-nitro PAH isomers products listed in Table 1 by calculating their dipole
161 moments using Gaussian with B3LYP/6-31G(d) (Table SI.2) and predicted the molecular ion of
162 the NCI mass spectra based on their molecular weight.

163 *Benzo[a]pyrene.* Figures SI.1A-C show the NCI full scan chromatograms of BaP-d₁₂

164 exposed to NO₂, NO₃/N₂O₅, and OH radical overlaid with the chromatogram of the unexposed
165 BaP-d₁₂. The m/z 264 peak is the molecular ion of BaP-d₁₂. Because the extracts from the
166 unexposed filters were split, in some cases, the parent PAH peaks in the unexposed extracts had
167 lower abundances than those in the exposed extracts. BaP-d₁₂ reacted with NO₂ and NO₃/N₂O₅
168 (Figures SI.1A and SI.1B) and yielded significant amounts of mono NO₂-BaP-d₁₁ isomers. In
169 contrast, after the OH radical exposures, noticeably lower amounts of mono NO₂-BaP-d₁₁
170 products were formed (Figures SI.1C). Three mono NO₂-BaP-d₁₁ isomers (Figures SI.1A-C,
171 peaks 1-3) were identified from the reaction of BaP-d₁₂ with NO₂, NO₃/N₂O₅, and OH radicals
172 (Table 1). No dinitro PAH isomers were identified in the BaP-d₁₂ exposures. Based on the ΔG
173 values shown in Table 1, we predicted that the most reactive position for OH attack of BaP was
174 6, followed by 1 and 3, respectively. This prediction was consistent with a previous study which
175 determined the distribution of NO₂-BaP isomers based on the calculated reactivity numbers.³⁰
176 The calculated dipole moments of these isomers suggested a GC retention time order of 6-, 1-
177 and 3-NO₂-BaP-d₁₁ (Table SI.2) and this same retention time order was previously observed for
178 these isomers using the same type of nonpolar GC column.³¹ Therefore, the earliest eluting peak
179 with m/z 308 (Figures SI.1A and SI.1B, peak 1) was identified as 6-NO₂-BaP-d₁₁ and its
180 retention time was confirmed with a standard of 6-NO₂-BaP-d₁₁. This peak had the highest peak
181 height (~20-490 times higher than 1- and 3-NO₂-BaP-d₁₁), in both EI and NCI, and corresponded
182 to the highest stability of the calculated 6-OH-BaP adduct (Table 1). In addition, 6-NO₂-BaP was
183 recently identified as a major product from the heterogeneous reaction of BaP coated soot
184 particles with NO₂.¹⁴ A slight difference in dipole moments of 1- and 3-NO₂-BaP-d₁₁ (6.06 and
185 6.16 Debye, respectively) predicted close GC retention times for these two isomers and peaks 2
186 and 3 (both with m/z 308) were tentatively assigned to 1- and 3-NO₂-BaP-d₁₁, respectively. 1-

187 and 3-NO₂-BaP were previously found to be minor products from a study of heterogeneous
188 reaction of BaP with NO₂ and N₂O₅.^{8, 12} However, to date, 1- and 3-NO₂-BaP have not been
189 measured in the environment (Table 1).

190 *Benzo[k]fluoranthene*. Figures SI.2A-C show the NCI full scan chromatograms of BkF-
191 d₁₂ exposed to NO₂, NO₃/N₂O₅, and OH radical overlaid with the chromatogram of the
192 unexposed BkF-d₁₂. The m/z 264 peak is the molecular ion of BkF-d₁₂. Two mono NO₂-BkF-
193 d₁₁ peaks (m/z 308), 3- and 7-NO₂-BkF-d₁₁, were identified from the reaction of BkF-d₁₂ with
194 NO₂ (Figure SI.2A) based on the ΔG values shown in Table 1. The weaker calculated dipole
195 moment of 7-NO₂-BkF-d₁₁, relative to 3-NO₂-BkF-d₁₁, suggested it would elute first. The
196 retention time of 7-NO₂-BkF-d₁₁ was confirmed with the non-deuterated 7-NO₂-BkF standard,
197 noting a slight difference in retention times due to the deuterium isotope effect. Therefore, peaks
198 1 and 2 were identified as 7-NO₂- BkF-d₁₁ and 3-NO₂-BkF-d₁₁, respectively. The formation of 3-
199 NO₂-BkF-d₁₁ was expected to be more favorable than 7-NO₂-BkF-d₁₁ based on the stability of
200 the various OH-BkF adducts (Table 1). However, the intensity of the 3-NO₂-BkF-d₁₁ peak was
201 significantly lower than that of 7-NO₂-BkF-d₁₁. The same observation was made in the EI full
202 scan chromatogram and may suggest that 3-NO₂-BkF-d₁₁ was more prone to further nitration,
203 yielding di-NO₂-BkF-d₁₀, compared to 7-NO₂-BkF-d₁₁. BkF-d₁₂ was nitrated during the
204 NO₃/N₂O₅ exposure and five mono-NO₂-BkF-d₁₁ products (m/z 308) were tentatively identified
205 in the NCI full scan chromatogram (Figure SI.2B). As shown in Table 1, the predicted order of
206 product formation, based on the thermodynamic stability of the OH-BkF adducts, was: 3, 7, 8, 1
207 and 9 positions of mono-NO₂-BkF-d₁₁. Based on the calculated dipole moments of these
208 compounds, the predicted GC retention time elution order was: 7-, 1-, 8-, 3- and 9-NO₂-BkF-d₁₁
209 (Table SI.2). It should be noted that all of the extracts were also run in SIM mode and the mono-

210 NO₂-BaP-d₁₁ peaks were baseline resolved in the selected ion chromatograms (data not shown).

211 In addition to the mono-NO₂-BkF-d₁₁ products, di-NO₂-BkF-d₁₀ products (m/z 352) were
212 also identified after the NO₃/N₂O₅ exposure (Figure SI.2B). Dinitro-PAHs are believed to form
213 from reaction of mono-nitro PAHs with the oxidizing agent^{5,13} and, therefore, the predicted most
214 abundant mono-NO₂-BkF-d₁₁ product (3-NO₂-BkF-d₁₁), with the most stable OH-BkF-d₁₁
215 intermediate, was most likely to further react with an oxidizing agent. To predict the most likely
216 di-NO₂-BkF-d₁₀ products, we calculated the thermodynamic stability of the OH-3-NO₂-BkF-d₁₀
217 adducts. If 3-NO₂-BkF-d₁₁ were the only mono-NO₂-BkF-d₁₁ isomer that underwent further
218 nitration, the five dominant di-NO₂-BkF-d₁₀ products were predicted to be: 3,12-, 3,7-, 3,4-, 3,6-
219 and 3,8-NO₂-BkF-d₁₀ (Figure SI.3). Because 3-NO₂-BkF-d₁₁ was not the only mono-NO₂-BkF-
220 d₁₁ product formed, other di-nitro-BkF-d₁₀ isomers may also have been formed. The positive
221 identification of these di-NO₂-BkF-d₁₀ products required authentic standards which were not
222 commercially available. Only the identity of 3,7-NO₂-BkF-d₁₀ (peak 11) was confirmed with the
223 non-deuterated 3,7-NO₂-BkF standard.

224 The OH radical exposure chromatograms indicated the presence of 7, 3, 8, and 1-NO₂-
225 BkF-d₁₁, but not 9-NO₂-BkF-d₁₁ (Figure SI.2C). The NCI full scan chromatograms for OH
226 radical exposures showed traces of other degradation products, possibly oxygenated PAHs,
227 mostly eluting before the mono-NO₂-BkF-d₁₁ and di-NO₂-BkF-d₁₀ isomers (Figures SI.2C). To
228 date, the mono-NO₂-BkF and di-NO₂-BkF isomers identified in this study have not been
229 measured in the environment (Table 1).

230 *Benzo[ghi]perylene*. Unlike the other PAHs, BghiP-d₁₂ was not effectively nitrated by
231 NO₂ and only one small unidentified peak (m/z 483) was observed in the NCI full scan
232 chromatogram (Figure SI.4A). In contrast, after NO₃/N₂O₅ exposure, three apparent mono-NO₂-

233 BghiP-d₁₁ isomers (m/z 332) were identified (Figure SI.4B). Based on the ΔG values shown in
234 Table 1, we predicted that 5-, 7-, and 4-NO₂-BghiP-d₁₁ would be the most abundant mono-NO₂-
235 BghiP-d₁₁ products. A previous study also identified 5-NO₂-BghiP as a dominant nitro product
236 formed from the reaction of BghiP adsorbed on silica gel particles with NO₂.¹⁶ The calculated
237 dipole moments suggested a retention time elution order of 7-, 4-, and 5-NO₂-BghiP-d₁₁ (Table
238 SI.2). After OH radical exposure, only 5-NO₂-BghiP-d₁₁, the predicted most abundant NO₂-
239 BghiP-d₁₁ isomer, was identified in the NCI full scan chromatogram (Figure SI.4C). To date, the
240 mono-NO₂-BghiP isomers identified in this study have not been measured in the environment
241 (Table 1).

242 *Dibenzo[a,i]pyrene.* As shown in Figures SI.5A and SI.5B, the NO₂ and NO₃/N₂O₅
243 exposures resulted in only one mono-NO₂-DaiP-d₁₃ product (m/z 360). Based on the ΔG values
244 shown in Table 1, we predicted that 5-NO₂-DaiP-d₁₃ would be the most abundant mono-NO₂-
245 DaiP-d₁₃ product. To date, 5-NO₂-DaiP has not been measured in the environment (Table 1). The
246 exposure of DaiP-d₁₄ to OH radicals did not result in any mono-NO₂-DaiP-d₁₃ products (Figures
247 SI.5C).

248 *Dibenzo[a,l]pyrene.* Because a perdeuterated DalP standard was not commercially
249 available, we used a nondeuterated DalP standard for our experiments. The presence of DalP in
250 a blank exposed filter was below the detection limit. A single mono-NO₂-DalP peak (m/z 347)
251 was observed after the NO₂ and NO₃/N₂O₅ exposures (Figure SI.6A and SI.6B). Based on the ΔG
252 values shown in Table 1, we predicted that 6-NO₂-DalP would be the most abundant mono-NO₂-
253 DalP product and, to date, 6-NO₂-DalP has not been measured in the environment (Table 1).
254 Similarly, OH radical exposure also resulted in the formation of a single mono-NO₂-DalP peak
255 (m/z 347), likely 6-NO₂-DalP, but to a much lesser extent than the NO₂ and NO₃/N₂O₅ exposures

256 (Figure SI.6C).

257 *Estimated Effectiveness of Nitration.* The percent of NPAH product formation relative to
258 the amount of unexposed parent PAH was calculated and used to estimate the effectiveness of
259 nitration for the different PAHs tested, under the various exposure conditions. We estimated the
260 percent of nitro product formation from the sum of identified NPAH product peak areas (in
261 exposed extracts) to its parent PAH peak area (in unexposed extracts) from the EI full scan
262 chromatograms (Table SI.3). These values should be considered rough estimates because the
263 objective of this research was to qualitatively identify nitro products and not quantitatively
264 determine their concentrations (there was no surrogate addition for quantitation). BaP-d₁₂ was
265 the most readily nitrated, in comparison to the other PAHs tested, by the NO₂, NO₃/N₂O₅ and OH
266 radical exposures (90%, 41%, and 20%, respectively), while BghiP-d₁₂ was the least effectively
267 nitrated (Table SI.3). Among the various exposures, the percent NPAH product formation was
268 highest for the NO₂ exposures.

269 **Salmonella Mutagenicity Assay.** Spontaneous revertant counts of DMSO (30 µl) alone were
270 ~25/plate for both assays. The mutagenicity of the chamber air system was tested by placing
271 clean filters in all chamber experiments. In the assays without S9, the revertant counts for the
272 blank filters were 27, 38, and 28 revertants/plate for the NO₂, NO₃/N₂O₅, and OH exposures,
273 respectively. In the assays with S9, the revertant counts for the blank filters were 44, 42, and 35
274 revertants/plate for the NO₂, NO₃/N₂O₅, and OH exposures, respectively. Overall, they were
275 comparable to the spontaneous revertant counts. This shows that the chamber environment and
276 our sample preparation process had no substantial effect on the mutagenicity results. The split
277 extracts of the unexposed filters, containing ~1 nmol of the individual PAHs tested, resulted in
278 43 to 65 revertants/plate and 24 to 49 revertants/plate for the assays with and without S9,

279 respectively (Figure 1).

280 *Direct-acting mutagenicity.* Many NPAHs are direct-acting mutagens, independent of
281 metabolic activation³². Figure 1A shows the means and standard errors of the direct-acting
282 mutagenicity of the various exposure extracts. The direct-acting mutagenicity increased the most
283 after NO₃/N₂O₅ exposure, particularly for BkF-d₁₂. For all of the PAHs tested, the NO₃/N₂O₅
284 exposure resulted in 6- to 432-fold increase in the direct-acting mutagenicity. The sharp increase
285 in the direct-acting mutagenicity of the NO₃/N₂O₅ exposed BkF-d₁₂ (432-fold) extract may
286 correspond to the formation of the di-NO₂-BkF-d₁₀ products. The dose-response profiles of two
287 non-deuterated NO₂-BkF standards indicated that 3,7-NO₂-BkF is a strong direct-acting
288 mutagen, whereas 7-NO₂-BkF is not (Figure SI.7A). Higher mutagenic activities of di-NO₂-
289 PAH-d₁₀ products, in comparison to mono-nitro isomers, were reported for dinitropyrenes in
290 which their direct-acting mutagenicity, in TA98, was 272- to 467-fold higher than that of 1-
291 nitropyrene.³³

292 The increases in the direct-acting mutagenicity of BaP-d₁₂ were less pronounced after
293 exposure to NO₂ and OH radicals, compared to the NO₃/N₂O₅ exposure where the direct-acting
294 mutagenicity increased by 43-fold (Figure 1A). This sharp increase was due to the formation of
295 1- and 3-NO₂-BaP-d₁₁ products, rather than the formation of 6-NO₂-BaP-d₁₁ because 6-NO₂-
296 BaP-d₁₁ contains a nitro group perpendicular to the aromatic moiety.³⁴ Previous studies
297 suggested that NPAHs with a perpendicular orientation of the NO₂ group relative to the aromatic
298 plane, have a high first half-wave reduction potential, which restricts the nitro-reduction process
299 by bacteria.^{33, 34} A mixture of 1-NO₂-BaP and 3-NO₂-BaP was previously found to be 2.5 fold
300 more mutagenic with TA98, than 6-NO₂-BaP.⁸ Some studies have reported that 1- and 3-NO₂-
301 BaP were direct-acting mutagens in a Salmonella assay, but 6-NBaP was not.^{35, 36} In a more

302 recent study, 1- and 3-NO₂-BaP were found to induce 713 and 1,931 revertants/nmol,
303 respectively, in TA98, while 6-NO₂-BaP induced less than 1 revertant/nmol.³³ However, the
304 direct-acting mutagenicity of the NO₂ exposed BaP-d₁₂ extract was surprisingly low given that
305 the same mono-NO₂-BaP-d₁₁ products were measured as in the NO₃/N₂O₅ exposure (Figures 1A
306 and SI.1A) and the percent NPAH formation was the highest (Table SI.3). We confirmed that
307 this was not due to cytotoxicity. Therefore, the relatively high direct-acting mutagenicity of the
308 NO₃/N₂O₅ exposed BaP-d₁₂ extract may have been caused by the formation of other, yet
309 unidentified, products.

310 For BghiP-d₁₂, the direct-acting mutagenicity of the NO₂ exposed extract was not
311 significantly different from the unexposed extract. This finding was consistent with the chemical
312 analysis which showed insignificant NPAH formation after the NO₂ exposure. However, there
313 were 97 and 12-fold increases in the direct-acting mutagenicity after BghiP-d₁₂ was exposed to
314 NO₃/N₂O₅ and OH radicals, respectively (Figure 1A), corresponding to the formation of mono-
315 NO₂-BghiP-d₁₁ products. Of the three identified mono-NO₂-BghiP-d₁₁ products, 7-NO₂-BghiP-
316 d₁₁ is expected to contribute the least to the direct-acting mutagenicity due to the NO₂ orientation
317 (Table SI.4). Dose-response profiles of non-deuterated 5-NO₂-BghiP and 7-NO₂-BghiP
318 standards showed that both were non-mutagenic (< 1 rev/nmol) (Figure SI.7).

319 Changes in direct-acting mutagenicity of DaiP-d₁₄ and DalP with the different exposures
320 were less pronounced than the other PAHs tested (Figure 1A), suggesting that the single nitro
321 product formed did not exhibit strong direct-acting mutagenicity. The orientation of nitro
322 groups in both 5-NO₂-DaiP-d₁₄ and 6-NO₂-DalP, identified as the major products from all
323 exposures, are nearly perpendicular to the aromatic plane (Table SI.4) and may cause these
324 products to be less mutagenic.

325 *Indirect-acting mutagenicity.* Unsubstituted PAHs are known to be indirect-acting
326 mutagens which require metabolic activation to express mutagenicity and unreacted parent PAHs
327 may contribute to the indirect-acting mutagenicity of exposed extracts. In addition, not all
328 NPAHs are direct-acting mutagens. For example, 6-NO₂-BaP was previously found to be an
329 indirect-acting mutagen^{36, 37} and some NPAHs, including 1-NO₂-BaP and 3-NO₂-BaP, exhibit
330 both direct- and indirect-acting mutagenicity.³⁶ As shown in Figure 1B, the overall indirect-
331 acting mutagenicity profile was similar to the direct-acting mutagenicity profile, with
332 increased indirect-acting mutagenicity after the NO₃/N₂O₅ exposures. This shows that NO₃/N₂O₅
333 are not only strong oxidants in transforming PAHs to NPAHs, but also in forming potential direct
334 and indirect-acting mutagens. In particular, BaP-d₁₂, BkF-d₁₂, and BghiP-d₁₂ were degraded to
335 both strong direct-acting and strong indirect-acting mutagenic products. BkF-d₁₂ and BghiP-d₁₂
336 were the only two compounds that induced indirect-acting mutagenic activities significantly
337 higher than the background after OH radical exposure (Figure 1B and Figure SI.8B). Dose-
338 response profiles of non-deuterated 7-NO₂-BkF and 3,7-NO₂-BkF standards showed that the 3,7-
339 NO₂-BkF exhibited both direct- and indirect-acting mutagenicity (96 and 513 rev/nmol,
340 respectively), while 7-NO₂-BkF was not mutagenic in either assay (Figure SI.7). This implies
341 that the presence of the five di-NO₂-BkF-d₁₁ products in the NO₃/N₂O₅ exposed extract
342 contributed significantly to the direct-acting mutagenicity, as well as the indirect-acting
343 mutagenicity. On the other hand, 5-NO₂-BghiP was mutagenic to TA98 with S9 (27 rev/nmol),
344 while 7-NO₂-BghiP was not (Figure SI.7).

345 *Deuterium Isotope Effect on Mutagenicity.* The results from the deuterium isotope effect
346 mutagenicity studies of BaP/BaP-d₁₂, 6-NO₂-BaP/6-NO₂-BaP-d₁₁, PYR/PYR-d₁₀ and 1-NO₂-
347 PYR/1-NO₂-PYR-d₉ are shown in Figures SI.9A-D and Figures SI.10A-D. ANOVA analysis was

348 carried out to determine the statistical significance of differences between deuterated and non-
349 deuterated pairs of PAHs. There was no statistically significant deuterium isotope effect
350 (ANOVA, $P > 0.05$) for the parent BaP/BaP-d₁₂ and PYR/PYR-d₁₀ in the direct acting
351 mutagenicity assay (Figures SI.9A and SI.10A). However, a statistically significant deuterium
352 isotope effect (ANOVA, $P < 0.05$) was observed for 6-NO₂-BaP/6-NO₂-BaP-d₁₁ and 1-NO₂-
353 PYR/1-NO₂-PYR-d₉ (Figures SI.9C and SI.10C) in the direct acting mutagenicity assay. While
354 6-NO₂-BaP exhibited a weak direct-acting mutagenicity, the activity of 6-NO₂-BaP-d₁₁ was
355 comparable to the background response (Figure SI.9C). GC/MS analysis of the 6-NO₂-BaP
356 standard, with both EI and NCI, showed no contamination of 3- and/or 1-NO₂-BaP. However,
357 both 1-NO₂-PYR and 1-NO₂-PYR-d₉ were direct acting mutagens. The difference in the
358 magnitudes of the deuterium isotope effect on the direct-acting mutagenicity of 1-NO₂-PYR/1-
359 NO₂-PYR-d₉ and 6-NO₂-BaP/6-NO₂-BaP-d₁₁ cannot be explained by this study alone. Additional
360 studies on other NPAHs and/or the use of different bacterial strains may help to understand the
361 difference in the metabolic pathways.

362 In the indirect acting mutagenicity assay, no statistically significant deuterium isotope
363 effect was observed for the parent BaP/BaP-d₁₂ and PYR/PYR-d₁₀ (ANOVA, $P > 0.05$) (Figure
364 SI.9B and SI.10B). However, a statistically significant deuterium isotope effect was observed for
365 6-NO₂-BaP/6-NO₂-BaP-d₁₁ and 1-NO₂-PYR/1-NO₂-PYR-d₉ in the indirect acting mutagenicity
366 assay (ANOVA, $P < 0.05$) and substitution of deuterium for hydrogen lowered the mutagenicity
367 (Figures SI.9D and SI.10D). Overall, the deuterium isotope effect study suggested that
368 substitution of deuterium for hydrogen lowered the direct and indirect acting mutagenicity of
369 NPAHs and may result in an underestimation of the mutagenicity of the novel NPAHs identified
370 in this study. Further discussion is provided in the SI.

371 **Acknowledgements**

372 This publication was made possible in part by grant number P30ES00210 from the
373 National Institute of Environmental Health Sciences (NIEHS), NIH and NIEHS Grant P42
374 ES016465, and the U.S. National Science Foundation (ATM-0841165). Its contents are solely
375 the responsibility of the authors and do not necessarily represent the official view of the NIEHS,
376 NIH. Salmonella assays were conducted in the Cancer Chemoprotection Program (CCP) Core
377 Laboratory of the Linus Pauling Institute, Oregon State University.

378 **Supporting Information Available**

379 This material is available free of charge via the Internet at <http://pubs.acs.org>.

380 **References**

- 381
- 382 1. Atkinson, R.; Arey, J., Atmospheric Chemistry of Gas-Phase Polycyclic Aromatic
- 383 Hydrocarbons: Formation of Atmospheric Mutagens. *Environ. Health Perspect.* **1994**, *102*, 117-
- 384 126.
- 385 2. Durant, J. L.; Lafleur, A. L.; Plummer, E. F.; Taghizadeh, K.; Busby, W. F.; Thilly, W.
- 386 G., Human Lymphoblast Mutagens in Urban Airborne Particles. *Environ. Sci. Technol.* **1998**, *32*,
- 387 1894-1906.
- 388 3. Purohit, V.; Basu, A. K., Mutagenicity of Nitroaromatic Compounds. *Chem. Res.*
- 389 *Toxicol.* **2000**, *13*, 673-692.
- 390 4. Atkinson, R.; Arey, J.; Zielinska, B.; Aschmann, S. M., Kinetics and Nitro-Products of
- 391 the Gas-Phase OH and NO₃ Radical-Initiated Reactions of Naphthalene-d₈, Fluoranthene-d₁₀,
- 392 and Pyrene. *Int. J. Chem. Kinet.* **1990**, *22*, 999-1014.
- 393 5. Zimmermann, K.; Jariyasopit, N.; Massey Simonich, S. L.; Tao, S.; Atkinson, R.; Arey,
- 394 J., Formation of Nitro-PAHs from the Heterogeneous Reaction of Ambient Particle-Bound PAHs
- 395 with N₂O₅/NO₃/NO₂. *Environ. Sci. Technol.* **2013**, *47*, 8434-8442.
- 396 6. Zielinska, B.; Arey, J.; Atkinson, R.; Ramdahl, T.; Winer, A. M.; Pitts, J. N., Reaction of
- 397 dinitrogen pentoxide with fluoranthene. *J. Am. Chem. Soc.* **1986**, *108*, 4126-4132.
- 398 7. Zimmermann, K.; Atkinson, R.; Arey, J.; Kojima, Y.; Inazu, K., Isomer distributions of
- 399 molecular weight 247 and 273 nitro-PAHs in ambient samples, NIST diesel SRM, and from
- 400 radical-initiated chamber reactions. *Atmos. Environ.* **2012**, *55*, 431-439.
- 401 8. Pitts Jr, J. N.; Van Cauwenberghe, K. A.; Grosjean, D.; Schmid, J. P.; Fitz, D. R.; Belser,
- 402 W.; Knudson, G.; Hynds, P. M., Atmospheric reactions of polycyclic aromatic hydrocarbons:
- 403 facile formation of mutagenic nitro derivatives. *Science (New York, NY)* **1978**, *202*, 515-519.

- 404 9. Zelenyuk, A.; Imre, D.; Beránek, J.; Abramson, E.; Wilson, J.; Shrivastava, M., Synergy
405 between secondary organic aerosols and long-range transport of polycyclic aromatic
406 hydrocarbons. *Environ. Sci. Technol.* **2012**, *46*, 12459-12466.
- 407 10. Kamens, R. M.; Guo, J.; Guo, Z.; McDow, S. R., Polynuclear aromatic hydrocarbon
408 degradation by heterogeneous reactions with N₂O₅ on atmospheric particles. *Atmos. Environ.*
409 **1990**, *24*, 1161-1173.
- 410 11. Esteve, W.; Budzinski, H.; Villenave, E., Relative rate constants for the heterogeneous
411 reactions of NO₂ and OH radicals with polycyclic aromatic hydrocarbons adsorbed on
412 carbonaceous particles. Part 2: PAHs adsorbed on diesel particulate exhaust SRM 1650a. *Atmos.*
413 *Environ.* **2006**, *40*, 201-211.
- 414 12. Pitts, J. N.; Sweetman, J. A.; Zielinska, B.; Atkinson, R.; Winer, A. M.; Harger, W. P.,
415 Formation of nitroarenes from the reaction of polycyclic aromatic hydrocarbons with dinitrogen
416 pentoxide. *Environ. Sci. Technol.* **1985**, *19*, 1115-1121.
- 417 13. Miet, K.; Le Menach, K.; Flaud, P. M.; Budzinski, H.; Villenave, E., Heterogeneous
418 reactivity of pyrene and 1-nitropyrene with NO₂: Kinetics, product yields and mechanism.
419 *Atmos. Environ.* **2009**, *43*, 837-843.
- 420 14. Carrara, M.; Wolf, J.-C.; Niessner, R., Nitro-PAH formation studied by interacting
421 artificially PAH-coated soot aerosol with NO₂ in the temperature range of 295-523 K. *Atmos.*
422 *Environ.* **2010**, *44*, 3878-3885.
- 423 15. Pitts Jr, J. N.; Zielinska, B.; Sweetman, J. A.; Atkinson, R.; Winer, A. M., Reactions of
424 adsorbed pyrene and perylene with gaseous N₂O₅ under simulated atmospheric conditions.
425 *Atmos. Environ.* **1985**, *19*, 911-915.

- 426 16. Delmas, S.; Muller, J. F., Use of FTMS laser microprobe for the in situ characterization
427 of nitro-PAHs on particles. *Analisis*. **1992**, *20*, 165-170.
- 428 17. Bamford, H. A.; Baker, J. E., Nitro-polycyclic aromatic hydrocarbon concentrations and
429 sources in urban and suburban atmospheres of the Mid-Atlantic region. *Atmos. Environ.* **2003**,
430 *37*, 2077-2091.
- 431 18. Wang, W.; Jariyasopit, N.; Schrlau, J.; Jia, Y.; Tao, S.; Yu, T.-W.; Dashwood, R. H.;
432 Zhang, W.; Wang, X.; Simonich, S. L. M., Concentration and Photochemistry of PAHs, NPAHs,
433 and OPAHs and Toxicity of PM_{2.5} during the Beijing Olympic Games. *Environ. Sci. Technol.*
434 **2011**, *45*, 6887-6895.
- 435 19. Albinet, A.; Leoz-Garziandia, E.; Budzinski, H.; Villenave, E., Polycyclic aromatic
436 hydrocarbons (PAHs), nitrated PAHs and oxygenated PAHs in ambient air of the Marseilles area
437 (South of France): Concentrations and sources. *Sci. Total Environ.* **2007**, *384*, 280-292.
- 438 20. Hattori, T.; Tang, N.; Tamura, K.; Hokoda, A.; Yang, X.; Igarashi, K.; Ohno, M.; Okada,
439 Y.; Kameda, T.; Toriba, A., Particulate polycyclic aromatic hydrocarbons and their nitrated
440 derivatives in three cities in Liaoning Province, China. *Environ. Forensics* **2007**, *8*, 165-172.
- 441 21. USEPA *Development of a Relative Potency Factor (RPF) Approach for Polycyclic*
442 *Aromatic Hydrocarbon (PAH) Mixtures, an external review draft*; U.S. Environmental
443 Protection Agency, Intergrated Risk Information System (IRIS): Washington, DC, 2010.
- 444 22. Devanesan, P. D.; Cremonesi, P.; Nunnally, J. E.; Rogan, E. G.; Cavalieri, E. L.,
445 Metabolism and mutagenicity of dibenzo [a, e] pyrene and the very potent environmental
446 carcinogen dibenzo [a, l] pyrene. *Chem. Res. Toxicol.* **1990**, *3*, 580-586.

- 447 23. Pitts Jr, J. N.; Zielinska, B.; Sweetman, J. A.; Atkinson, R.; Winer, A. M., Reactions of
448 adsorbed pyrene and perylene with gaseous N₂O₅ under simulated atmospheric conditions.
449 *Atmos. Environ.* **1967**, *19*, 911-915.
- 450 24. Maron, D. M.; Ames, B. N., Revised methods for the Salmonella mutagenicity test.
451 *Mutat. Res.* **1983**, *113*, 173-215.
- 452 25. Pitts Jr, J. N.; Sweetman, J. A.; Zielinska, B.; Winer, A. M.; Atkinson, R., Determination
453 of 2-nitrofluoranthene and 2-nitropyrene in ambient particulate organic matter: Evidence for
454 atmospheric reactions. *Atmos. Environ.* **1985**, *19*, 1601-1608.
- 455 26. Zimmermann, K.; Atkinson, R.; Arey, J., Effect of NO₂ Concentration on
456 Dimethylnitronaphthalene Yields and Isomer Distribution Patterns from the Gas-Phase OH
457 Radical-Initiated Reactions of Selected Dimethylnaphthalenes. *Environ. Sci. Technol.* **2012**, *46*,
458 7535-7542.
- 459 27. Miet, K.; Le Menach, K.; Flaud, P. M.; Budzinski, H.; Villenave, E., Heterogeneous
460 reactivity of pyrene and 1-nitropyrene with NO₂: Kinetics, product yields and mechanism.
461 *Atmos. Environ.* **2009**, *43*, 837-843.
- 462 28. Gross, S.; Bertram, A. K., Reactive uptake of NO₃, N₂O₅, NO₂, HNO₃, and O₃ on three
463 types of polycyclic aromatic hydrocarbon surfaces. *J. Phys. Chem. A* **2008**, *112*, 3104-3113.
- 464 29. White, C.; Robbat, A.; Hoes, R., Gas chromatographic retention characteristics of nitrated
465 polycyclic aromatic hydrocarbons on SE-52. *Chromatographia* **1983**, *17*, 605-612.
- 466 30. Dewar, M.; Mole, T.; Urch, D.; Warford, E., 689. Electrophilic substitution. Part IV. The
467 nitration of diphenyl, chrysene, benzo [a] pyrene, and anthanthrene. *J. Chem. Soc.* **1956**, 3572-
468 3575.

469 31. Bamford, H. A.; Bezabeh, D. Z.; Schantz, M. M.; Wise, S. A.; Baker, J. E.,
470 Determination and comparison of nitrated-polycyclic aromatic hydrocarbons measured in air and
471 diesel particulate reference materials. *Chemosphere* **2003**, *50*, 575-587.

472 32. Fu, P. P., Metabolism of nitro-polycyclic aromatic hydrocarbons. *Drug Metab. Rev.*
473 **1990**, *22*, 209-268.

474 33. Jung, H.; Heflich, R. H.; Fu, P. P.; Shaikh, A. U.; Hartman, P., Nitro group orientation,
475 reduction potential, and direct-acting mutagenicity of nitro-polycyclic aromatic hydrocarbons.
476 *Environ. Mol. Mutagen.* **1991**, *17*, 169-180.

477 34. Fu, P. P.; Qui, F. Y.; Jung, H.; Von Tungeln, L. S.; Zhan, D. J.; Lee, M. J.; Wu, Y. S.;
478 Heflich, R. H., Metabolism of isomeric nitrobenzo[a]pyrenes leading to DNA adducts and
479 mutagenesis. *Mutat. Res.* **1997**, *376*, 43-51.

480 35. Chou, M.; Heflich, R.; Casciano, D.; Miller, D.; Freeman, J.; Evans, F.; Fu, P., Synthesis,
481 spectral analysis, and mutagenicity of 1-, 3-, and 6-nitrobenzo [a] pyrene. *J. Med. Chem.* **1984**,
482 *27*, 1156-1161.

483 36. Pitts Jr, J. N.; Zielinska, B.; Harger, W. P., Isomeric mononitrobenzo [a] pyrenes:
484 synthesis, identification and mutagenic activities. *Mutat. Res.* **1984**, *140*, 81-85.

485 37. Rosenkranz, H. S.; Mermelstein, R., The mutagenic and carcinogenic properties of
486 nitrated polycyclic aromatic hydrocarbons. In White, C. M., Ed. Huethig: Heidelberg, 1985; pp
487 267-297.

488 38. Schauer, C.; Niessner, R.; Pöschl, U., Analysis of nitrated polycyclic aromatic
489 hydrocarbons by liquid chromatography with fluorescence and mass spectrometry detection: air
490 particulate matter, soot, and reaction product studies. *Anal. Bioanal. Chem.* **2004**, *378*, 725-736.
491

492 **Scheme 1.** General mechanism for the nitration of PAHs via gas-phase reaction with OH radical.

493 **Table 1.** Free energies (ΔG_{rxn}) of OH-PAH adducts calculated using density functional theory
494 (B3LYP) and the 6-31G(d) basis set, list of NPAHs measured in the laboratory studies, and
495 whether or not the NPAH have been to date identified in the environment. The NPAH isomers
496 are listed in order of predicted expected abundance.

497 **Figure 1.** Mean (\pm standard error) of A) direct-acting and B) indirect-acting mutagenicities
498 (revertants/plate) of filter extracts. All extracts were tested in triplicate for mutagenic activity.

499

500

501

502

503

504

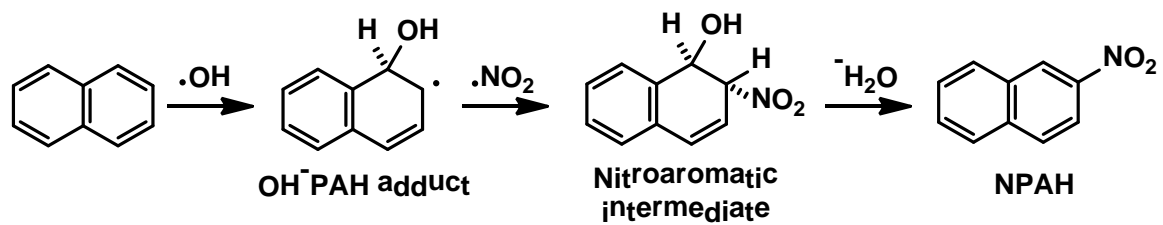
505

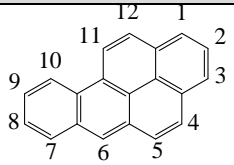
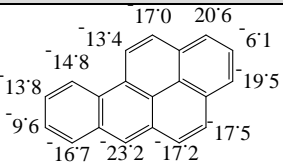
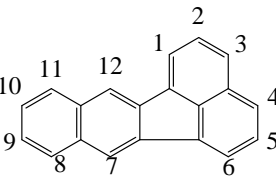
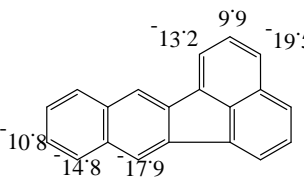
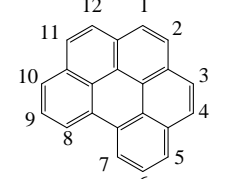
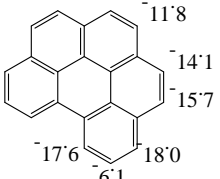
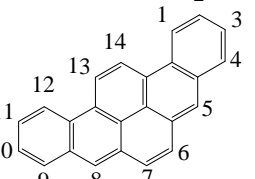
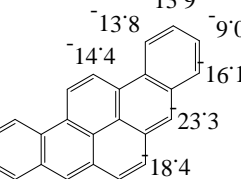
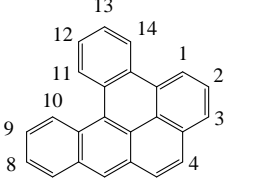
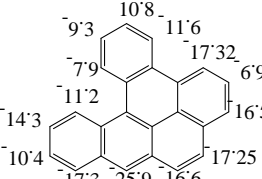
506

507

508

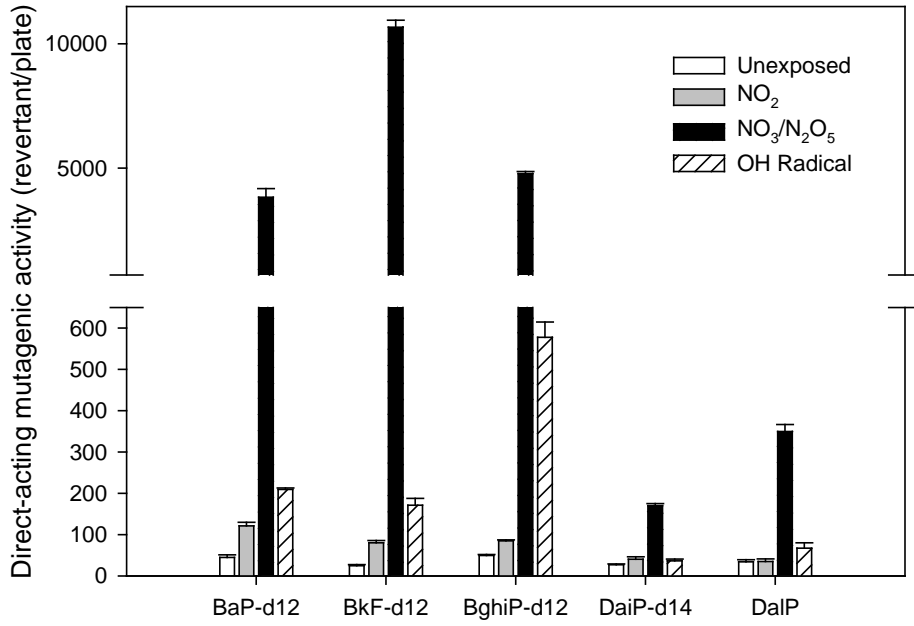
509



PAH Studied	Numbering Scheme	Predicted OH-PAH-Adduct ΔG_{rxn} (Kcal/mol)	NPAH products identified in laboratory experiments	Laboratory exposures NPAH were identified in [±]	Previously detected in environment?
Benzo[a]pyrene			6-nitrobenzo[a]pyrene ^ψ 1-nitrobenzo[a]pyrene [*] 3-nitrobenzo[a]pyrene [*]	NO ₂ , NO ₃ /N ₂ O ₅ , OH NO ₂ , NO ₃ /N ₂ O ₅ , OH NO ₂ , NO ₃ /N ₂ O ₅ , OH	Y ^{17, 19, 20, 38} N N
Benzo[k]fluoranthene			3-nitrobenzo[k]fluoranthene [*] 7-nitrobenzo[k]fluoranthene ^θ 8-nitrobenzo[k]fluoranthene [*] 1-nitrobenzo[k]fluoranthene [*] 9-nitrobenzo[k]fluoranthene [*] 3,7-dinitrobenzo[k]fluoranthene ^θ 4 dinitrobenzo[k]fluoranthenes [*]	NO ₂ , NO ₃ /N ₂ O ₅ , OH NO ₂ , NO ₃ /N ₂ O ₅ , OH NO ₃ /N ₂ O ₅ , OH NO ₃ /N ₂ O ₅ , OH NO ₃ /N ₂ O ₅ NO ₃ /N ₂ O ₅ NO ₃ /N ₂ O ₅	N N N N N N N
Benzo[ghi]perylene			5-nitrobenzo[ghi]perylene ^θ 7-nitrobenzo[ghi]perylene ^θ 4-nitrobenzo[ghi]perylene [*]	NO ₃ /N ₂ O ₅ , OH NO ₃ /N ₂ O ₅ NO ₃ /N ₂ O ₅	N N N
Dibenzo[a,i]pyrene			5-nitrodibenzo[a,i]pyrene [*]	NO ₂ , NO ₃ /N ₂ O ₅	N
Dibenzo[a,l]pyrene			6-nitrodibenzo[a,l]pyrene [*]	NO ₂ , NO ₃ /N ₂ O ₅ , OH	N

^ψ verified with deuterated standard. ^θ verified with non-deuterated standard. [±]Perdeuterated forms were measured in the experiments. * Not verified, no standards available.

A.



B.

